Available online at www.sciencedirect.com
SCIENCE DIRECT®
Talanta 65 (2005) 313–323
Talanta
www.elsevier.com/locate/talanta

Optical biosensor for pharmaceuticals, antibiotics, hormones, endocrine disrupting chemicals and pesticides in water: Assay optimization process for estrone as example

Jens Tschmelak*, Guenther Proll, Guenter Gauglitz

Institute of Physical and Theoretical Chemistry (IPTC), Eberhard-Karls-University of Tuebingen, Auf der Morgenstelle 8, D-72076 Tuebingen, Germany

Received 27 November 2003; received in revised form 15 January 2004; accepted 2 July 2004
Available online 27 August 2004

Abstract

Certain contaminants at trace concentrations in surface waters can have dramatic effects on the hormonal system of organisms in the aquatic environment. Therefore, immunoanalytical methods at a very low limit of detection (LOD) and a low limit of quantification (LOQ) are becoming more and more important for environmental analysis and especially for monitoring drinking water quality. Environmental monitoring of antibiotics, hormones, endocrine disrupting chemicals, and pesticides in real water samples (e.g. surface, ground or drinking water) with difficult matrices places high demands on chemical analysis. Biosensors have suitable characteristics such as efficiency in allowing very fast, sensitive, and cost-effective detection. Here we describe an assay optimization process with a fully automated immunoassay for estrone which resulted in a LOD below 0.20 ng L^{-1} and a LOQ below 1.40 ng L^{-1}. In contrast to common analytical methods such as GC–MS or HPLC–MS, the biosensor used requires no sample pre-treatment and pre-concentration. The very low validation parameters for estrone are the result of the continuous optimization of the immunoassay. The basis of our sensitive assay is the antibody with a high affinity constant towards estrone. During the optimization process, we reduced the amount of antibody per sample and improved the chip surface modification. Finally, this proceeding led to a calibration routine with an amount of antibody of only 3.0 ng per sample (sample volume: 1.0 mL). The reduction of the amount of antibody per sample results in better validation parameters (LOD, LOQ, and IC_{50}), but this reduction leads to the current device-related limitation of the River Analyser (RIANA).

For some endocrine disrupting compounds, no effect levels (NOELs) in the lower nanogram per liter range are reported. This defines the challenge, which analytical methods have to compete with and our RIANA instrument with its improved sensitivity for the detection of a single hormone in the lower nanogram per liter range is a powerful tool in aquatic analytics in addition to the common analytical methods.

Keywords: River Analyser (RIANA); Automated Water Analyser Computer Supported System (AWACSS); Hormones; Estrogenic compounds; Endocrine disrupting chemicals; Environmental analysis; Assay optimization

1. Introduction

Immunoanalytical methods at a very low limit of detection (LOD) and a low limit of quantification (LOQ) are becoming more and more important for environmental analysis and especially for monitoring drinking water quality. In recent years, immunoassays have been improved significantly and here we want to describe a fully automated immunosensor based on total internal reflection fluorescence (TIRF) which can measure several organic compounds (pharmaceuticals, antibiotics, hormones, endocrine disrupting chemicals, and pesticides) in parallel. In this case, we used the automated immunoassay to measure estrone as example of a group of estrogenic compounds. The antibody used can detect not only estrone but also several other estrogenic compounds such as 17α-ethinylestradiol, 17β-estradiol, diethylstilbestrol or estriol. Throughout the scientific world, the hypothesis has been put forward that humans and wildlife species suffer adverse

* Corresponding author. Tel.: +49 7071 2974668; fax: +49 7071 295490.
E-mail address: jens.tschmelak@ipc.uni-tuebingen.de (J. Tschmelak).
URL: http://www.barolo.ipc.uni-tuebingen.de.

0039-9140/$ – see front matter © 2004 Elsevier B.V. All rights reserved.
doi:10.1016/j.talanta.2004.07.011

health effects after exposure to endocrine disrupting compounds. Reported adverse effects include declines in populations, increases in cancers, and reduced reproductive function [10]. A huge amount of natural hormones and endocrine disrupting chemicals are reaching surface waters [22,14,4]. The main sources of this pollution are wastewater treatment plants and intensive stock rearing. Estrogenic compounds and the effects of whose mixtures are not entirely clear, but a no effect concentration (NOEC) in the lower nanogram per liter range is often discussed in literature.

For β-estradiol experiments with juvenile rainbow trout has demonstrated that vitellogenin can be induced in this species after 14 days exposure to 4.7–7.9 ng L^{-1} 17β-estradiol [23]. NOEC was in another study of the same author assessed to <5 ng L^{-1} [24]. Less studies have in general been performed with both estrone and estriol compared to the other natural estrogen, 17β-estradiol. The lowest observable effect concentration (LOEC) for estrone in regard to vitellogenin synthesis has been reported to be 3.2 ng L^{-1} for juvenile female rainbow trout [31] after an exposure period of 14 days. Ten times as high a LOEC of 31.8 ng L^{-1} was found for vitellogenin synthesis in male fathead minnow after 21 days of exposure [16] which compares well with a LOEC of between 25 and 50 ng L^{-1} for adult male rainbow trout exposed for the same period of time [21]. Estrone is widely considered to be of similar or slightly lower in vivo estrogenic potency than 17β-estradiol as also seen from the above-mentioned experiments. An up to five times lower potency of estrone has been suggested [29]. The potency of estriol in regard to vitellogenin induction in male fish has not been determined by water exposure experiments. Estriol is in general considered to be the least estrogenic of the three natural estrogens. An in vitro study has demonstrated estriol to be 30 times less potent than 17β-estradiol [24]. A number of studies have examined the feminizing potential of the synthetic estrogen, 17α-ethinylestradiol on various endpoints. The NOEC for vitellogenin in fish has been tested in numerous species [26,19,7,1,20,27]. The lowest concentration which has been found to induce vitellogenin in male fish is 0.1 ng L^{-1} (nominal concentration) after exposure of adult male rainbow trout for 10 days [19]. Other studies with zebra fish and rainbow trout have reported vitellogenin induction at 1–5 ng L^{-1} 17α-ethinylestradiol in short-term exposure experiments [8,26,7,1,20]. This agrees with the general finding that rainbow trout is the more sensitive of a number of test species with regard to vitellogenin induction [20]. In conclusion, LOECs for vitellogenin and intersex induction by 17α-ethinylestradiol are very low observed at concentrations of 0.1 ng L^{-1} and a wide range of testicular effects have been seen at concentrations from 1 to 10 ng L^{-1}. This illustrates that 17α-ethinylestradiol is even more potent in regard to feminization of male fish than β-estradiol.

Analytical methods at a low LOD and LOQ for problematic compounds in water are very important in environmental analysis [10]. For common analytical methods like GC–MS and HPLC–MS it is necessary to pre-concentrate samples by orders of magnitude to reach detectable amounts of the analytes [17]. To overcome the problems in sample pretreatment and to reduce the costs, immunoassays such as the enzyme-linked immunosorbent assay (ELISA) have been developed. The applications for ELISA in environmental monitoring are limited, because up to now it was not possible to automate this technique for routine analysis [28]. Other attempts to automate a flow injection immunoaffinity analysis (FIIAA) system as a screening technology for atrazine and diuron have been described [12]. Our fully automated optical biosensor River Analyser (RIANA) uses labeled antibodies to detect specific organic analytes in water samples without pre-concentration [11,2]. This sensor can be used as a very fast and cost-effective instrument for surveillance and early warning in environmental analysis. Long-term stability tests of the biosensor surface showed that over 400 measurements including regeneration cycles are possible, which verified the robustness of our optical sensor system.

Up to now, no routine analytical method for environmental monitoring of water samples based on an immunoassay has been published. Therefore, we developed an optical biosensor for pharmaceuticals, antibiotics, hormones, endocrine disrupting chemicals, and pesticides in water with difficult matrices. To reach a very low LOD and a low LOQ for various analytes each of the assays has to be optimized. The immunoassay for estrone resulted in a LOD below 0.20 ng L^{-1} and a LOQ below 1.40 ng L^{-1} which has been published in a short communication [25]. Here we want to report the assay optimization process and the systematic assay validation for estrone as example with all-important factors of influence and the device-related limits.

2. Experimental

2.1. Materials

Common chemicals of analytical grade were purchased from Sigma, Deisenhofen, Germany, or Merck KGaA, Darmstadt, Germany. The estrogenic compounds estrone (1,3,5(10)-estratrien-3-ol-17-one), diethylstilbestrol ((E)-3,4-bis(4-hydroxyphenyl)-3-hexene), estriol (1,3,5(10)-estratriene-3,16α,17β-triol), 17β-estradiol (1,3,5-estratriene-3,17β-diol), and 17α-ethinylestradiol (17α-ethinyl-1,3,5-estratriene-3,17β-diol) were purchased in form of VETRANAL® analytical standards from Riedl-de Haën Laborchemikalien GmbH & Co. KG, Seelze, Germany. The fluorescent dye CyDye™ Cy5.5 was purchased from Amersham Biosciences Europe GmbH, Freiburg, Germany, and the fluorescent dye Alexa Fluor® 680 was purchased from Molecular Probes Europe BV, Leiden, The Netherlands. The aminodextrans Amdex™ with 40 and 170 K Dalton molecular weight were purchased from Helix Research Company, Springfield, OR, USA. Dr. Ram Abuknesha, King's College London, UK, kindly supplied the antibody anti-total-estrogen (a-ES) and the analyte

derivative employed in this study. Labeling and purification of antibody were carried out as described in the product information sheet supplied with the labeling kit from Amersham Biosciences Europe GmbH, Freiburg, Germany, and Molecular Probes Europe BV, Leiden, The Netherlands, respectively. UV–vis spectra were recorded using a Specord M500 spectrophotometer from Carl Zeiss Jena GmbH, Jena, Germany. The spatially resolved surface modification was performed using a piezoelectric ink-jet system from Microdrop GmbH, Norderstedt, Germany.

2.2. Instrumentation

The setup of the River Analyser (RIANA) is shown in Fig. 1a and consists of the following components [2]: light from a laser diode (Coherent Deutschland GmbH, Dieburg, Germany) with 15 mW operating at 635 nm is coupled into the beveled edge of a bulk optical glass slide (Schott Spezialglas GmbH, Gruenenplan, Germany). The laser beam is guided by total internal reflection along the sensitive area of the glass transducer. Fluorescent dyes near to the chip surface are excited by the evanescent field of the reflection spots. The emitted light is collected by polymer optical fibers, filtered by absorption filters with cut-on at 700 nm (Omega® Optical Inc., Brattleboro, VT, USA) and detected by photo diodes using lock-in detection. An HTC PAL auto sampler with cycle composer software (CTC Analytics AG, Zwingen, Switzerland) is used for dilutions, sample preparations (transferring 100 μL of the antibody stock solution to 900 μL of the sample followed by one or two mixing strokes) and the sample transfer to the River Analyser. Liquid handling and data acquisition are fully automated and computer controlled. One measurement cycle with washing steps, injection of the sample and regeneration of the surface takes about 12 min.

2.3. Methods

The test format used for all measurements is a binding inhibition assay shown in Fig. 1b. Here an analyte derivative (analyte molecule modified with a spacer containing a carboxyl group) is covalently immobilized to an aminodextran layer bound to the glass transducer. This aminodextran layer is used to reduce non-specific binding to the surface. Dried aminodextran layers on a glass substrate showed a thickness between 1 and 3 nm. The thickness of welled aminodextran layers were also verified by spectroscopic ellipsometry experiments and these experiments yielded values between 100 and 150 nm. The sample containing the analyte is incubated in solution with the labeled specific antibody. Therefore, 100 μL of the antibody stock solution are mixed with 900 μL of the sample by an auto sampler and are incubated for approximately 5 min. The antibody binds the analyte during the incubation step until the equilibrium of the reaction is reached. When the sample is pumped over the sensor surface, only the antibodies with free binding sites can bind to the surface. For the binding inhibition assay to be quantitative, the binding of the antibody to the surface must be mass transport-limited. This allows the signal to be a function of rather the diffusion rate to the surface then of the kinetics of the surface binding. The number of high affinity binding sites on the surface has to be much higher than the number of antibodies used for one measurement. To be sure, that the binding is mass transport-limited, we use small amounts of antibodies and on the sensor surface we immobilize a huge excess of antigen derivatives. This was demonstrated by additional reflectometric interference spectroscopy (RIfS) measurements as already described in literature [5]. The surface evaluation was performed with covalently immobilized peptide nucleic acid (PNA) for the detection of different endocrine disruptors by the abovementioned label-free detection method. Within these experiments, a hybridization capacity with DNA oligonucleotides of 180 fmol mm^{-2} on PNA-surfaces has been reported [13]. Other experiments to evaluate a covalent strategy for immobilization of DNA-microspots suitable for microarrays with label-free and time-resolved optical detection of hybridization resulted in hybridization capacities of approximately 300 fmol mm^{-2} [9]. Fig. 6 shows the achieved linear correlation between the increasing fluorescence signal and the antibody concentration used for simple TIRF experiments. The linear behavior of the fluorescence signal shows that no saturation effects can be observed even with highest antibody concentrations. Therefore, the immobilized huge excess of antigen derivatives in comparison to the used amounts of antibodies could be verified.

The binding inhibition assay was carried out in single analyte operating state. For measuring only one analyte with one derivative on the surface, the complete sensitive area of the transducer can be modified with this derivative on the previously covalent bound aminodextran [18]. The establishing of multi-analyte transducers requires a spatially resolved surface chemistry protocol [2]. Nevertheless, we used this protocol to perform a single analyte transducer for estrone, because with this method we achieve a higher density of immobilized analyte derivatives on the surface. The two linear fits in Fig. 6 also show the advantage of the spatially resolved surface chemistry protocol.

2.4. Immobilization

Active esters were prepared with the derivatives, which are analyte molecules modified with a spacer containing a carboxyl group. Approximately 5.0 mg of the derivative were dissolved in 100 μL of dry *N*,*N*-dimethylformamide (DMF). *N*-hydroxysuccinimide (NHS) and *N*,*N*′-dicyclohexylcarbodiimide (DCC), each in 1.1-fold molar excess (referring to the amount of analyte derivative) were added to the solution. After stirring for several minutes, the solution was kept over night at room temperature. Finally, the solution was centrifuged (12,000 rpm) at approximately 4 °C and the supernatant was stored under refrigeration. 50 mg of aminodextran were dissolved in a mixture of 500 μL Milli-Q water and 500 μL DMF. The active ester solution was

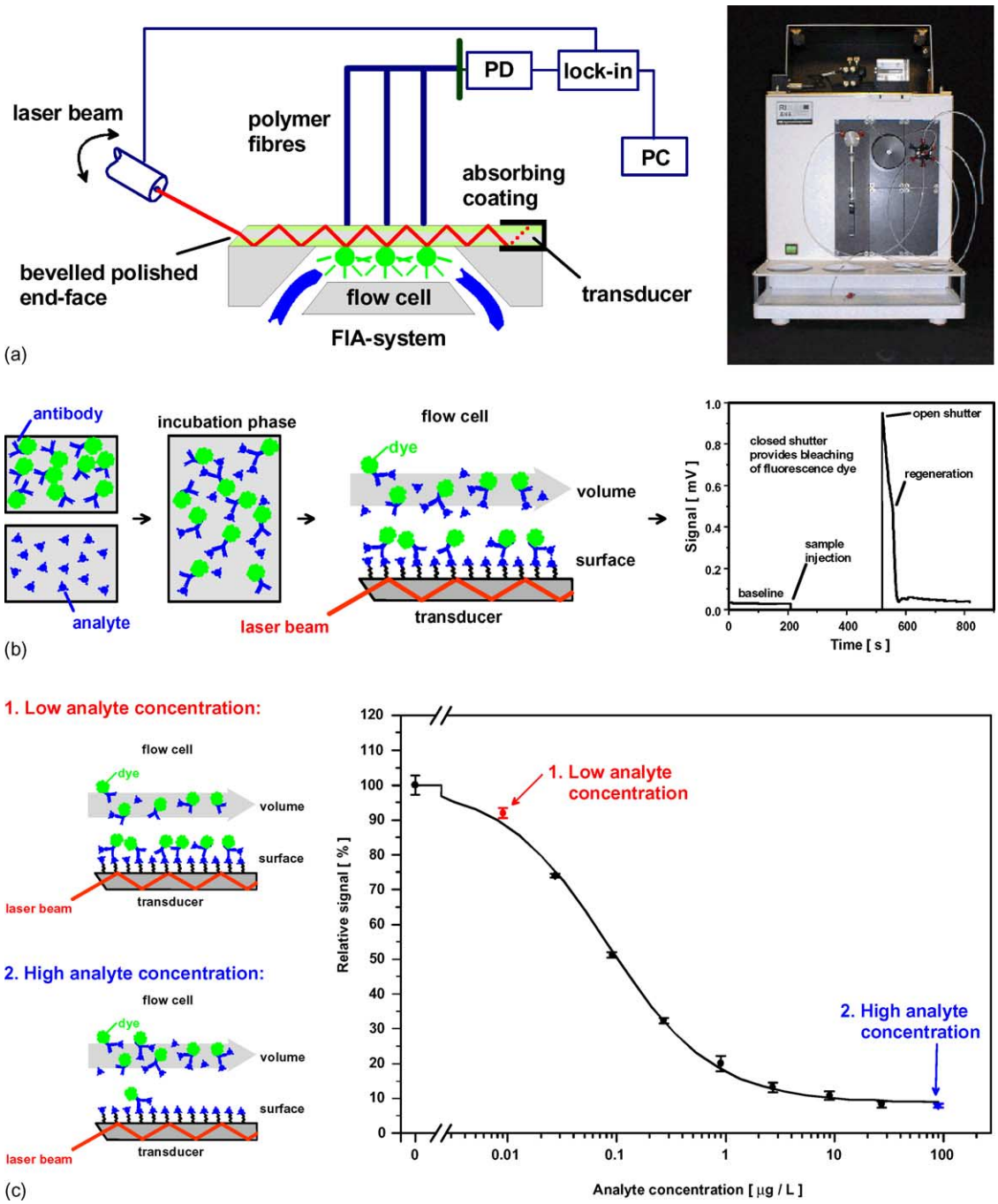

Fig. 1. (a) Schematic setup of the direct optical immunosensor RIANA (River Analyzer). The setup basically consists of a laser diode, a transducer, a flow cell, a FIA-system combined with an auto sampler, polymer fibers, filters, photo diodes (PD), a lock-in, and a personal computer (PC). (b) Principle of the binding inhibition assay with the sample (containing the analyte) and the antibody stock solution, incubation phase and the sensor surface with immobilized analyte derivatives. The result of an individual measurement is shown as an example of data acquisition. (c) Schematic measurements for a low analyte concentration (1) and a high analyte concentration (2) which result in different signals for the logistic fit of a calibration curve.

added, mixed thoroughly and kept over night at room temperature. A tenfold volume excess of methanol precipitated the aminodextran conjugate. The supernatant was removed and the conjugate was freeze-dried. The glass transducers were cleaned in a freshly prepared mixture of hydrogen peroxide and concentrated sulphuric acid (ratio 2:3) for up to 30 min and rinsed with Milli-Q water. After drying under a nitrogen flow, 25 μL of (3-glycidyloxypropyl)trimethoxysilane (GOPTS) were applied to the surface and reacted for up to 60 min. The silanized surface was rinsed with dry acetone and dried under a flow of nitrogen. Subsequently, the aminodextran conjugates were dissolved in Milli-Q water at a concentration of 2.0 mg mL^{-1} and were immobilized by an ink-jet dispenser. The remaining area between the (separate) detec-

tion spots was covered with non-conjugated aminodextran to prevent non-specific antibody binding [18].

The immobilization in spatially distinct loci required a micro-dispensing device. The core of the MicroDrop® (Microdrop GmbH, Norderstedt, Germany) micro-dispenser system used consists of a glass capillary, which is surrounded by a piezo actuator. Applying a voltage pulse to the piezo, it contracts and creates a pressure pulse in the liquid inside the capillary. At the nozzle the pressure is transferred into a highly accelerated motion which expels a small droplet. This droplet flies with a velocity of 1.5–3.0 m s^{-1}. Typical drop diameters are 30–100 μm depending on the nozzle diameter. Volume variation is less than 1%. On the sensor surface up to six spots can be spotted in a row within the middle of the flow cell. Each spot has a 3 mm diameter and consists of over 3000 single droplets from the micro-dispensing device used.

2.5. Measurement and data evaluation

For the measurements, we used a polyclonal IgG antibody from sheep and a suitable analyte derivative. The entire sample volume was 1 mL, and the total amount of labeled antibody for a single measurement was between 120 and 3 ng. For a calibration routine, 900 μL of spiked Milli-Q water was automatically mixed by the auto sampler with 100 μL of an antibody stock solution containing the antibodies and ovalbumin from chicken eggs (OVA) in 10-fold phosphate buffered saline (PBS) (10-fold PBS: pH 6.8, 1500 mM sodium chloride, 100 mM potassium phosphate monobasic). After a defined incubation time this mixture was measured using the biosensor setup.

The experimental design for a calibration routine consists of 12 independent blank (Milli-Q water) measurements and nine concentration steps (each measured as three replica) of the analyte (spiked Milli-Q water). For all concentration steps and the blank measurements (12 replica) the mean value and the standard deviation (S.D.) for the replica was calculated. The measured signal for the mean value of the blanks was set to 100% and all spiked samples could be obtained as a relative signal below this blank value. To fit the dataset a logistic fit function Eq. (1) [3] (parameters of a logistic function: A_1, A_2, x_0, and p) with three free parameters (A_2, x_0, and p) was used.

$$y = \frac{A_1 - A_2}{1 + (x/x_0)^p} + A_2 \quad (1)$$

A_1, as the upper asymptote was fixed to 100% (relative signal for mean value of the blanks) and A_2 is the lower asymptote. The range between A_1 and A_2 is the dynamic signal range. The inflection point is given by the variable x_0 and represents the analyte concentration, which corresponds to a decrease of 50% of the dynamic signal range (IC_{50}). The slope of the tangent in this point is given by the parameter p. Schematic measurements for a low and a high analyte concentration, which result in different signals for the logistic fit of a calibration curve, are shown in Fig. 1c. The working range (for this kind of calibration curve) is often given by the 10–90% block of the dynamic signal range. Another possibility to determine the working range is to calculate the precision profile ($X_{cv,i}$) and its intersections with the Horwitz curve [6,15]. Based on scores of AOAC intercomparison programs, Horwitz developed an empiric correlation between the comparative standard deviation and the concentration. For laboratory

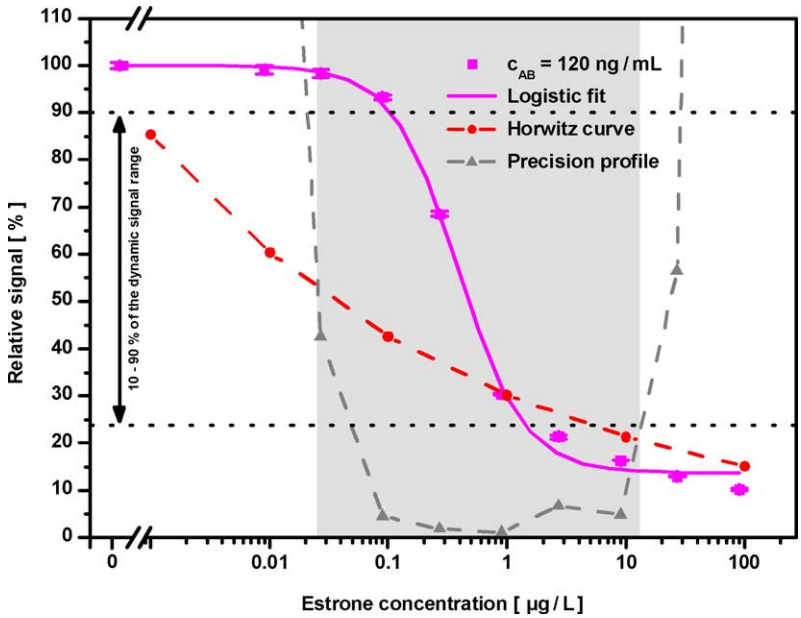

Fig. 2. Typical calibration curve for estrone measured on an E_{13}CME (derivative) modified surface from 0 to 90 μg L^{-1} (nine steps) as example. The antibody (a-ES) concentration (c_{AB}) was 120 ng mL^{-1}, the OVA concentration 0.25 mg mL^{-1} in each sample. Working range: 10–90% block of the dynamic signal range (dotted lines) vs. the method depending on the Horwitz curve and the precision profile (grey shaded area).

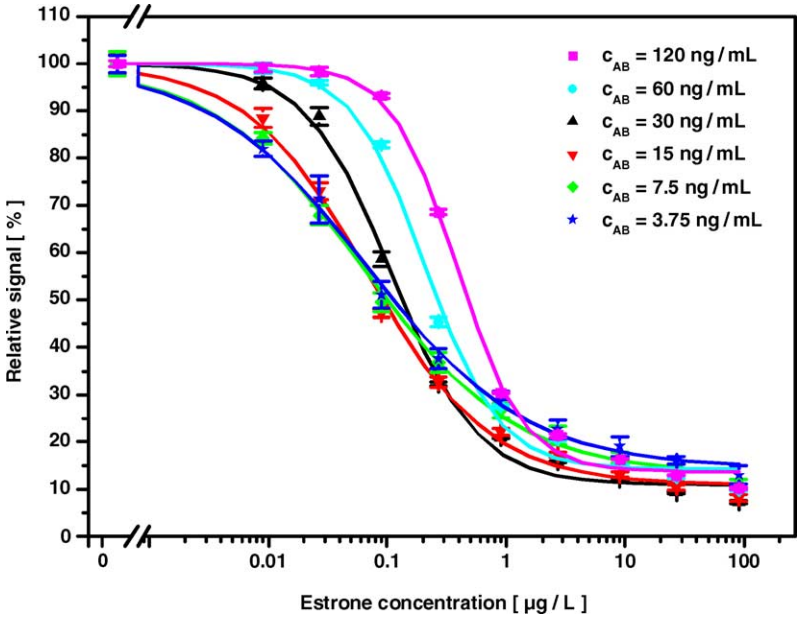

Fig. 3. Summary of the calibration curves for estrone measured with the E_{13}CME derivative on the surface from 0 to 90 $\mu g\,L^{-1}$ (nine steps). The antibody (a-ES) concentration (c_{AB}) was between 120 and 3.75 $ng\,mL^{-1}$, the OVA concentration 0.25 $mg\,mL^{-1}$ in each sample.

intercomparison programs Horwitz proposed a equation for the reproducibility σ_R Eq. (2) with a factor $f = 0.02$.

$$\sigma_R = f \times c^{0.8495} \quad (2)$$

The corresponding error is the relative standard deviation (R.S.D.) (Eq. (3)) which can be calculated with the reproducibility σ_R and the analyte concentration c.

$$\text{R.S.D.} = 100 \times \frac{\sigma_R}{c} \quad (3)$$

For an intra-laboratory reproducibility Horwitz found a higher precision and consequently lower R.S.D. values. Then the factor f can be reduced to two-thirds up to half of its former value. R.S.D. values can be calculated for each concentration and they represent the Horwitz curve in Figs. 2 and 3.

A valid concentration determination is possible only if the precision profile is below the Horwitz curve. The S.D. values of the inverse function (S.D.X_i) can be calculated using the S.D. values of the measured data (S.D.Y_i) and the associated values of the first derivative (Y') of the logistic fit (Y) for each concentration. Then the variation coefficients ($X_{cv,i}$) can be calculated and plotted together with the values of the Horwitz curve and the calibration data in the semi-logarithmic graph. Finally, the working range is given by the range between the intersection points of the Horwitz curve and the precision profile as can be seen in the example of Fig. 2. In this graph, the narrow working range determined using the 10–90% block of the dynamic signal range (dotted lines) is compared to the broader working range determined with the method depending on the Horwitz curve and the precision profile (grey shaded area).

In compliance with the IUPAC rules (orange book), the LOD is calculated as three times the S.D. of the blank measurements (S.D.$_{blanks}$) and the LOQ is calculated as 10 times the S.D. of the blank measurements (S.D.$_{blanks}$).

3. Results and discussion

In a first step, a freshly prepared single analyte transducer with the derivative E_{13}CME immobilized on the complete sensitive area of the chip was calibrated with estrone. This transducer was modified with the derivative E_{13}CME on the previously covalent bound aminodextran layer [18]. The calibration was performed from 0 to 90 $\mu g\,L^{-1}$ in nine concentration steps (0.009, 0.027, 0.09, 0.27, 0.9, 2.7, 9.0, 27.0 and 90.0 $\mu g\,L^{-1}$). The first calibration with 120 ng anti-total-estrogen (a-ES) per sample resulted in a perfect signal-to-noise ratio (SNR) of over 1400 for the blank measurements. The SNR was calculated with the mean error of the baselines as noise and the mean value of all blank measurements as signal. The error of each single concentration step (three replica) could be calculated between 0.05 and 0.98% (S.D.). The error of the blank measurements (12 replica) was 0.69% (S.D.$_{blanks}$). This first calibration with an amount of antibody of 120 ng per sample resulted in a LOD of 35.98 $ng\,L^{-1}$, a LOQ of 80.81 $ng\,L^{-1}$, an IC_{50} of 0.387 ± 0.025 $\mu g\,L^{-1}$, and a SNR of 1478 (signal: 151.44 µm, noise: 0.10 µV). The dataset, the logistic fit function, the precision profile, and the Horwitz curve were plotted in a semi-logarithmic graph as depicted (as example) in Fig. 2.

All validation parameters for the first calibration showed too high values for an application as a fully automated immunoassay in drinking water monitoring. Therefore, we halved the amount of antibody per sample and performed a new calibration with estrone. This calibration with an

Table 1
Parameters of the logistic fit function (A_2, x_0, and p) and the corresponding errors (S.D.A_2, S.D.x_0, and S.D.p) for all seven calibration curves with the different antibody concentrations (c_{AB}) between 3.0 and 120 ng mL^{-1} of anti-total-estrogen (a-ES)

Parameters	c_{AB} (ng mL^{-1})	A_2 (%)	S.D.A_2 (%)	x_0[a] (μg L^{-1})	S.D.x_0 (μg L^{-1})	p (μg L^{-1})	S.D.p (μg L^{-1})
No. 1[b]	120	13.70	1.28	0.387	0.025	1.561	0.128
No. 2[b]	60	14.24	1.79	0.209	0.020	1.399	0.167
No. 3[b]	30	10.95	1.43	0.109	0.009	1.199	0.105
No. 4[b]	15	10.93	1.35	0.069	0.006	0.844	0.060
No. 5[b]	7.5	13.07	1.27	0.064	0.006	0.675	0.042
No. 6[b]	3.75	14.40	1.29	0.067	0.006	0.647	0.040
No. 7[c]	3.0	17.16	1.54	0.062	0.004	0.639	0.052

[a] Parameter x_0 from the logistic fit function which represents the IC_{50}.
[b] Calibration range 0–90 μg L^{-1} estrone (nine steps).
[c] Calibration range 0–9 μg L^{-1} estrone (nine steps).

amount of antibody of 60 ng per sample resulted in a LOD of 13.95 ng L^{-1}, a LOQ of 34.28 ng L^{-1}, an IC_{50} of 0.209 ± 0.020 μg L^{-1}, and a SNR of 779 (signal: 74.99 μV, noise: 0.10 μV). Calculations resulted in an error of the concentration steps between 0.14 and 1.11% (S.D.) and an error of the blank measurements of 0.63% (S.D.$_{blanks}$).

Still the validation parameters should be improved and as a result, we reduced the amount of antibody to 30 ng per sample and performed a third calibration with estrone. An acceptable value for the IC_{50} within an assay for estrone would be approximately 0.05–0.07 μg L^{-1}. This third calibration resulted in a LOD of 4.71 ng L^{-1}, a LOQ of 13.48 ng L^{-1}, an IC_{50} of 0.109 ± 0.009 μg L^{-1}, and a SNR of 467 (signal: 39.16 μV, noise: 0.08 μV). The errors of the concentration steps were between 0.15 and 1.84% (S.D.) and the error of the blank measurements was 0.67% (S.D.$_{blanks}$).

The first success in reaching a LOD below 10 ng L^{-1}, a LOQ below 15 ng L^{-1}, and an IC_{50} close to 0.1 μg L^{-1} encouraged us to perform further measurements at lower antibody concentrations. Once again, we halved the amount of antibody per sample and performed a new estrone calibration with an amount of antibody of 15 ng per sample, which resulted in a LOD of 3.08 ng L^{-1}, a LOQ of 16.01 ng L^{-1}, an IC_{50} of 0.069 ± 0.006 μg L^{-1}, and a SNR of 235 (signal: 17.45 μV, noise: 0.08 μV). The errors of the concentration steps were between 0.51 and 1.98% (S.D.) and the error of the blank measurements was 2.01% (S.D.$_{blanks}$). In this step, the further reduction of the amount of antibody resulted in a lower LOD and a lower IC_{50} at a still practical SNR.

A further bisection of the amount of antibody to 7.5 ng per sample resulted (within a new calibration for estrone) in a LOD of 1.94 ng L^{-1}, a LOQ of 16.75 ng L^{-1}, an IC_{50} of 0.064 ± 0.006 μg L^{-1}, and a SNR of 117 (signal: 9.16 μV, noise: 0.08 μV). The errors of the concentration steps were between 0.59 and 2.08% (S.D.) and the error of the blank measurements was 2.51% (S.D.$_{blanks}$). With this calibration, we only reached a reduction of the LOD from 3.08 to 1.94 ng L^{-1} and a slightly lower IC_{50}.

Nevertheless, a calibration with only 3.75 ng anti-total-estrogen (a-ES) per sample was performed and resulted in a LOD of 1.07 ng L^{-1}, a LOQ of 9.06 ng L^{-1}, an IC_{50} of 0.067 ± 0.006 μg L^{-1}, and a SNR of 56 (signal: 4.72 μV, noise: 0.08 μV). The errors of the concentration steps were between 0.83 and 5.00% (S.D.) and the error of the blank measurements was 1.84% (S.D.$_{blanks}$). The partly huge errors for the concentration steps and the low signal-to-noise ratio (SNR) showed the device-related limits with the labeled antibody and the modified transducer used.

The total dataset of the six calibrations was used to calculate the validation parameters (LOD and LOQ) in compliance with the IUPAC rules (orange book). Table 1 is a summary of the parameters of the logistic fit functions (A_2, x_0, and p) including the corresponding errors (S.D.A_2, S.D.x_0, and S.D.p). Table 2 is a summary of the validation parameters

Table 2
Validation parameters (S.D.$_{blanks}$, LOD, LOQ, and IC_{50}) for all seven calibration curves with the different antibody concentrations (c_{AB}) between 3.0 and 120 ng mL^{-1} of anti-total-estrogen (a-ES)

Validation parameter	c_{AB} (ng mL^{-1})	S.D.$_{blanks}$ (%)	LOD (ng L^{-1})	LOQ (ng L^{-1})	IC_{50}[a] (ng L^{-1})
No. 1[b]	120	0.69	35.98	80.81	387 ± 25
No. 2[b]	60	0.63	13.95	34.28	209 ± 20
No. 3[b]	30	0.67	4.71	13.48	109 ± 9
No. 4[b]	15	2.01	3.08	16.01	69 ± 6
No. 5[b]	7.5	2.51	1.94	16.75	64 ± 6
No. 6[b]	3.75	1.84	1.07	9.06	67 ± 6
No. 7[c]	3.0	0.67	0.19	1.39	62 ± 4

[a] Parameter x_0 from the logistic fit function which represents the IC_{50}.
[b] Calibration range 0–90 μg L^{-1} estrone (nine steps).
[c] Calibration range 0–9 μg L^{-1} estrone (nine steps).

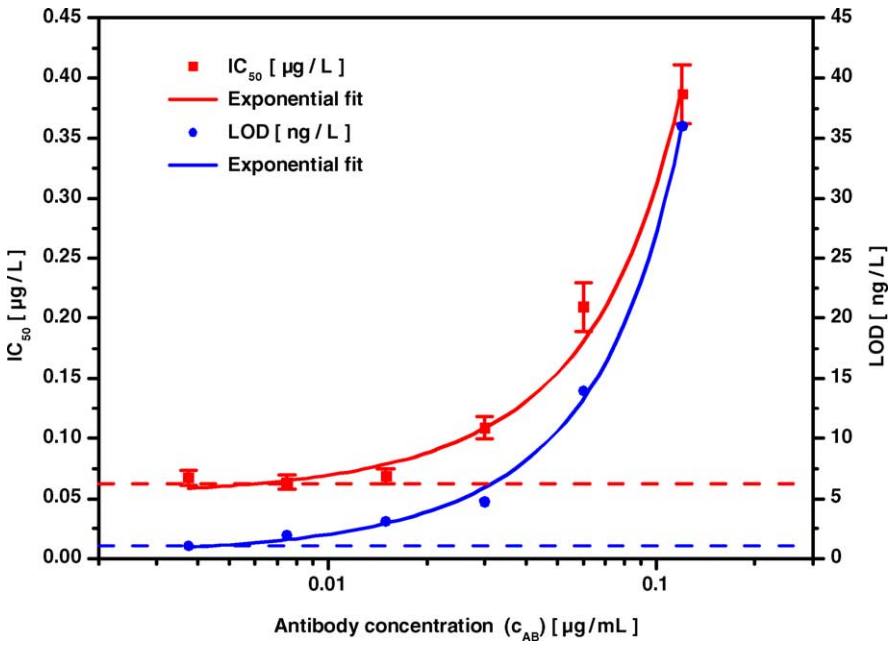

Fig. 4. Semi-logarithmic graph of the validation parameters LOD and IC_{50} of the six calibration curves for estrone (antibody concentration (c_{AB}) between 3.75 ng mL^{-1} and 0.12 μg mL^{-1}). The validation parameters were fitted with an exponential function separately.

($S.D._{blanks}$, LOD, LOQ, and IC_{50}) for all calibration curves. In Fig. 3 the six calibration curves with the different antibody concentrations (c_{AB}) between 3.75 and 120 ng mL^{-1} of anti-total-estrogen (a-ES) are collected in one graph. Fig. 4 shows the correlation between the used amount of antibody per sample and the validation parameters LOD and IC_{50}. Each dataset (LOD and IC_{50}) was fitted separately with an exponential function to illustrate the device-related limitation of an amount of antibody reduction. Generally, the best antibody concentration range must be adjusted to the requirements of the planned immunoassay application. For our field of applications the lowest antibody concentration with acceptable errors and the lowest limit of detection is the main target. For other applications (such as determining the analyte concentration of real water samples with different matrices) the antibody concentration should be adjusted to a range where the highest slope of the logistic fit function can be found in the analyte concentration range of interest.

In a second step, a freshly prepared single analyte transducer with an immobilized analyte derivative E_{13}CME on each spot was calibrated with estrone. The establishing of the new chip required a spatially resolved surface chemistry protocol [2], since using this method it is possible to achieve a higher density of immobilized analyte derivatives on the surface. The number of binding sites is lower when the complete sensitive area of the chip is modified using an aminodextran, and afterwards modified using the derivative, because this covalently bound aminodextran (170 K) layer has fewer free amino groups left for the derivatization procedure. For the other immobilization procedure we used an aminodextran (40 K) with more amino groups, which in a first step was modified using the derivative. Such a modified dextran can be immobilized (with a high density) in spatially distinct loci on an activated glass substrate using a micro-dispensing device. The higher density of immobilized analyte derivatives can result in an as high fluorescence signal as with less amount of antibody or in an higher fluorescence signal at the same antibody concentration as it can be seen in Fig. 6. Finally, this procedure results in more binding sites per mm^2.

The calibration with the new chip was performed from 0 to 9 μg L^{-1} in nine concentration steps (0.0009, 0.0027, 0.009, 0.027, 0.09, 0.27, 0.9, 2.7, and 9.0 μg L^{-1}). Such a lower concentration range became necessary, because the validation parameters LOD and LOQ were expected in the lower nanogram per liter range (as already shown with the plane-modified chip). This new transducer was calibrated with only 3.0 ng anti-total-estrogen (a-ES) per sample and resulted in a LOD of 0.19 ng L^{-1}, a LOQ of 1.39 ng L^{-1}, an IC_{50} of 0.062 ± 0.004 μg L^{-1}, and a SNR of 47 (signal: 3.85 μV, noise: 0.08 μV). The errors of the concentration steps were between 0.79 and 4.76% (S.D.) and the error of the blank measurements was 0.67% ($S.D._{blanks}$). This calibration curve with an amount of antibody of only 3.0 ng per sample was plotted in a semi-logarithmic graph as depicted in Fig. 5. The related validation parameters ($S.D._{blanks}$, LOD, LOQ, and IC_{50}) are also in Table 2 (see line No. 7) and the associated parameters of the logistic fit functions (A_2, x_0, and p) including the corresponding errors ($S.D.A_2$, $S.D.x_0$, and $S.D.p$) are in Table 1 (see line No. 7). For the first time, a LOD below 0.20 ng L^{-1} and a LOQ below 1.40 ng L^{-1} was reached with a fully automated immunosensor. This improved sensitivity to detect a hormone in the lower nanogram per liter range this optical biosensor is a powerful tool in aquatic analytics in addition to the common analytical methods.

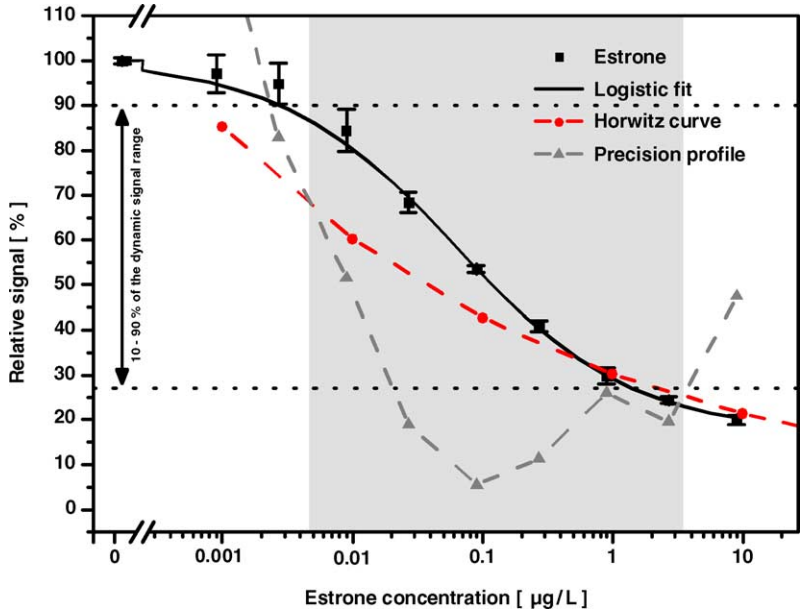

Fig. 5. Calibration curve for estrone measured on an E_{13}CME (derivative) modified surface from 0 to 9 µg L^{-1} (nine steps). The antibody (a-ES) concentration (c_{AB}) was 3.0 ng mL^{-1}, the OVA concentration 0.25 mg mL^{-1} in each sample. Working range: 10–90% block of the dynamic signal range (dotted lines) vs. the method depending on the Horwitz curve and the precision profile (grey shaded area).

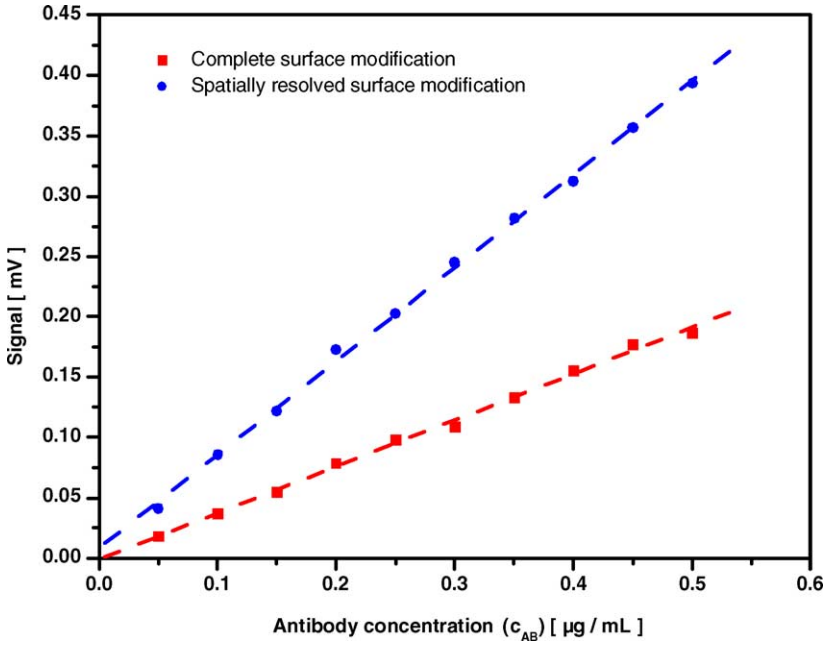

Fig. 6. Linear correlation between the increasing fluorescence signal and the antibody concentration used for simple TIRF experiments. These two linear fits show the advantage of the spatially resolved surface chemistry protocol (blue dotted line—dots) vs. the complete surface modification (red dotted line—squares).

To verify the calibration curve with the lowest LOD of 0.19 ng L^{-1} and to check the reproducibility, the precision, and the robustness of the sensor system spiked real water samples (0.27, 0.9, and 2.7 ng L^{-1} estrone in tap water) were measured. Two out of three recovery rates could be obtained between 70 and 120% in compliance with the AOAC International (Association of Analytical Communities). Only the recovery rate of the sample with the closest concentration (0.27 ng L^{-1}) to the LOD resulted in a value above 120% (typical overestimation of the biosensor setup used). The reproducibility was checked by measuring replica of each sample within independent repetitions. Robustness could be demonstrated by long-term stability tests of the biosensor surface.

4. Conclusions

Reducing the amount of antibody per sample resulted in better validation parameters (LOD, LOQ, and IC_{50}), but it also led to the current device-related limitation of the River Analyser (RIANA). For the first time, a LOD below 0.20 ng L^{-1} and a LOQ below 1.40 ng L^{-1} was reached with a fully automated immunoassay. Further improvements may need antibodies with a higher affinity constant and a higher labeling rate. Another possibility is the change of instrument components like the photo diodes (PD), the filters, the polymer fibers, and the laser diode, respectively. Up to now, the existing setup can be used as monitoring device for estrone. First measurements with real water samples containing estrone in the sub-nanogram per liter range could be determined with recovery rates between 70 and 120% as demanded by the AOAC International. This natural hormone was used as an example in the assay optimization process for a group of estrogenic compounds. The antibody (anti-total-estrogen) used can detected not only estrone, but also other problematic compounds like 17α-ethinylestradiol, 17β-estradiol, diethylstilbestrol, and estriol, respectively. Now the results of the optimized estrone assay have to be repeated with the other mentioned estrogenic compounds. One major problem for the simultaneous detection of the above-mentioned contaminents (in real water samples) is the cross-reactivity of the antibody (anti-total-estrogen) used. In future, a sum concentration determination for major estrogenic compounds in the environment with a LOD and LOQ in the lower nanogram per liter range might be possible. Then the immunosensor can be used to monitor aqueous samples from the environment or drinking water below the important no effect concentration (NOEC), which is often discussed in literature.

This fully automated immunosensor with its capability to measure not only estrone but also several other organic compounds like endocrine disrupting chemicals, endocrine disrupting compounds, hormones, pesticides, and antibiotics is therefore a perfectly suited instrument to serve as a low cost system for surveillance and early warning in environmental analysis. With its now improved sensitivity to detect a hormone in the lower nanogram per liter range this optical biosensor is a powerful tool in aquatic analytics in addition to the common analytical methods.

Acknowledgements

The main part of this work was funded by the "Automated Water Analyser Computer Supported System" (AWACSS) (EVK1-CT-2000-00045) research project supported by the European Commission under the Fifth Framework Program and contributing to the implementation of the Key Action "Sustainable Management and Quality of Water" within the Energy, Environment and Sustainable Development. Another part of this work has been supported by the Bundesministerium fuer Bildung und Forschung (BMBF) within the "Parallelisiertes immunreaktionsbasiertes Wasser-Analysator-System" (PIWAS) (FK-02WU0243-6) project. The development of the biosensor used was funded by the European Commission under the Environment and Climate Program River Analyser (RIANA) (ENV4-CT95-0066) project. Jens Tschmelak is a scholarship holder and Guenther Proll is participant of the research training group (Graduiertenkolleg) "Quantitative Analysis and Characterization of Pharmaceutically and Biochemically relevant Substances" funded by the Deutsche Forschungsgemeinschaft (DFG) at the Eberhard-Karls-University of Tuebingen. The mixture of polyclonal antibodies and the derivatives for the surface chemistry were kindly supplied by Dr. Ram Abuknesha, King's College London, London, UK.

References

[1] B. Allner, G. Wegener, T. Knacker, P. Stahlschmidt-Allner, Sci. Total Environ. 233 (1999) 21–31.
[2] C. Barzen, A. Brecht, G. Gauglitz, Biosens. Bioelectron. 17 (2002) 289–295.
[3] R.A. Dudley, P. Edwards, R.P. Ekins, D.J. Finney, I.G. McKenzie, G.M. Raab, D. Rodbard, R.P. Rodgers, Clin. Chem. 31 (1985) 1264–1271.
[4] H. Fukazawa, M. Watanabe, F. Shiraishi, H. Shiraishi, T. Shiozawa, H. Matsushita, Y. Terao, J. Health Sci. 48 (2002) 242–249.
[5] R.W. Glaser, Anal. Biochem. 213 (1993) 152–161.
[6] W. Horwitz, L.R. Kamps, K.W. Boyer, J. Assoc. Off. Anal. Chem. 63 (1980) 1344–1354.
[7] M. Islinger, D. Willimski, A. Volkl, T. Braunbeck, Aquat. Toxicol. 62 (2003) 85–103.
[8] S. Jobling, D. Sheahan, J.A. Osborne, P. Matthiessen, J.P. Sumpter, Environ. Toxicol. Chem. 15 (1996) 194–202.
[9] A. Jung, I. Stemmler, A. Brecht, G. Gauglitz, Fresenius J. Anal. Chem. 371 (2001) 128–136.
[10] R.J. Kavlock, G.P. Daston, C. DeRosa, P. Fenner-Crisp, L.E. Gray, S. Kaattari, G. Lucier, M. Luster, M.J. Mac, C. Maczka, R. Miller, J. Moore, R. Rolland, G. Scott, D.M. Sheehan, T. Sinks, H.A. Tilson, Environ. Health Persp. 104 (1996) 715–740.
[11] A. Klotz, A. Brecht, C. Barzen, G. Gauglitz, R.D. Harris, G.R. Quigley, J.S. Wilkinson, R.A. Abuknesha, Sens. Actuators B: Chem. 51 (1998) 181–187.
[12] P.M. Kraemer, A. Franke, C. Standfuss-Gabisch, Anal. Chim. Acta 399 (1999) 89–97.
[13] K. Kroeger, A. Jung, S. Reder, G. Gauglitz, Anal. Chim. Acta 469 (2002) 37–48.
[14] D.G.J. Larsson, M. Adolfsson-Erici, J. Parkkonen, M. Pettersson, A.H. Berg, P.-E. Olsson, L. Forlin, Aquat. Toxicol. 45 (1999) 91–97.
[15] V.R. Meyer, Schweizerische Laboratoriums-Zeitschrift 60 (2003) 63–65.
[16] G.H. Panter, R.S. Thompson, J.P. Sumpter, Aquat. Toxicol. 42 (1998) 243–253.
[17] M. Petrovic, E. Eljarrat, M.J. Lopez de Alda, D. Barcelo, J. Chromatogr. A 974 (2002) 23–51.
[18] J. Piehler, A. Brecht, K.E. Geckeler, G. Gauglitz, Biosens. Bioelectron. 11 (1996) 579–590.
[19] C.E. Purdom, P.A. Hardiman, V.J. Bye, N.C. Eno, C.R. Tyler, J.P. Sumpter, Chem. Ecol. 8 (1994) 275–285.
[20] J. Rose, H. Holbech, C. Lindholst, U. Norum, A. Povlsen, B. Korsgaard, P. Bjerregaard, Toxicol. Pharmacol. C 131 (2002) 531–539.
[21] E.J. Routledge, D. Sheahan, C. Desbrow, G.C. Brighty, M. Waldock, J.P. Sumpter, Environ. Sci. Technol. 32 (1998) 1559–1565.

[22] L.S. Shore, M. Gurevitz, M. Shemesh, Bull. Environ. Contamin. Toxicol. 51 (1993) 361–366.
[23] K.L. Thorpe, T.H. Hutchinson, M.J. Hetheridge, M. Scholze, J.P. Sumpter, C.R. Tyler, Environ. Sci. Technol. 35 (2001) 2476–2481.
[24] K.L. Thorpe, T.H. Hutchinson, M.J. Hetheridge, J.P. Sumpter, C.R. Tyler, Environ. Toxicol. Chem. 19 (2000) 2812–2820.
[25] J. Tschmelak, G. Proll, G. Gauglitz, Anal. Bioanal. Chem., in press (DOI: 10.1007/S00216-003-2357-4).
[26] K. Van den Belt, R. Verheyen, H. Witters, Arch. Environ. Contamin. Toxicol. 41 (2001) 458–467.
[27] K. Van den Belt, P.W. Wester, L.T.M. van der Ven, R. Verheyen, H. Witters, Environ. Toxicol. Chem./SETAC 21 (2002) 767–775.
[28] H.H. Weetall, Biosens. Bioelectron. 14 (1999) 237–242.
[29] W.F. Young, P. Whitehouse, I. Johnson, N. Sorokin, R&D Technical Report P2-T04/1, Environment Agency, Bristolm, UK, 2002.